Water Adsorption to Crystalline Cu_2O Thin Films – Structural and Vibrational Properties

C. Möller,[1] J. Barreto,[2] F. Stavale,[2] H. Tissot,[3] S. Shaikhutdinov,[3] H.J. Freund,[3]

N. Nilius [1,*]

[1] *Carl von Ossietzky Universität, Institut für Physik, D-26111 Oldenburg, Germany*

[2] *Brazilian Center for Research in Physics, Rio de Janeiro, Brazil*

[3] *Fritz-Haber-Institut der MPG, Faradayweg 4-6, D-14195 Berlin, Germany*

* *Corresponding author: University of Oldenburg, niklas.nilius@uni-oldenburg.de, phone +49-441-798-3152*

Abstract: D_2O adsorption to well-ordered $Cu_2O(111)$ thin films has been explored with scanning tunneling microscopy, thermal desorption and infrared absorption spectroscopy. The molecules bind associatively to the oxide surface, whereby the first D_2O layer experiences slightly stronger adhesion due to interfacial hydrogen bonds. At higher exposure, amorphous solid water (ASW) films condense on the $Cu_2O(111)$ surface, as concluded from a dominant desorption peak at 155 K. Development of ASW is also observed on bare Au(111), being used as substrate for Cu_2O growth. In contrast to the oxide surface, no binding enhancement is detected for the D_2O monolayer and desorption is accompanied by dewetting and transformation to crystalline ice. The different binding schemes of water reflect the hydrophilic versus hydrophobic nature of $Cu_2O(111)$ and Au(111) supports, respectively.

1 Introduction

Hydrophilicity and hydrophobicity are the fundamental counterparts of water-surface interactions in nature. While water-surface coupling as mediated by covalent bonding is stronger than intermolecular cohesion in the former case, hydrogen bonding inside the molecular network prevails in the latter.[1] Hydrophobicity results in the formation of 3D water structures and is often accompanied by a crystallization to ice.[2,3] Hydrophilic supports, on the other hand, exert a certain template effect on the water molecules that may result in ordered adsorption patterns. If the surface lattice deviates considerably from the intrinsic dimensions of the hydrogen-bonded network, ordering may be impeded and water condenses to amorphous films.[4] The formation of amorphous solid water, termed ASW in the following, may also arise from kinetic effects, e.g. when individual molecules are unable to reach their equilibrium arrangement despite a favorable energetic situation. In this case, gentle annealing may trigger the ice transition. Hydrophilicity is observed for many oxide surfaces, where both the cationic and anionic surface species are able to attract the water molecules.[5]

The exploration of H_2O crystallization phenomena has a long tradition and started already in the late 1970's.[6,7] Back then, the sharpening and redshift of characteristic vibrational bands have been taken as fingerprints for the transformation from ASW to ice. The main vibrational modes that are followed across the transition are the OH stretching, bending and libration modes. Their energetic position is readily detected with Raman and/or Fourier-transformed Infrared-Reflection Absorption Spectroscopy (FTIR). Assignment of the bands to specific inter- and intramolecular H_2O vibrations is however intricate and subject of ongoing theoretical modeling.[8,9,10] Also the molecular mechanisms behind the crystallization process are still in the focus of research.[11,12] With the advent of Scanning Tunneling Microscopy (STM), ordering effects in H_2O layers became accessible in real space.[2,4] Well-ordered water structures have been found on many metal and oxide supports, such as Pd(100), Ru(0001), FeO_x and CaO(100).[13,14,15] On Pt(111), dewetting phenomena and the development of ice clusters have been detected with molecular resolution, providing evidence for hydrophobic water-support interactions.[16,17]

In this study, we have examined the adsorption of water (D_2O) to crystalline Cu_2O films. Cuprous oxide has recently attracted much attention, because favorable optical properties make it interesting for

photocatalytic and photovoltaic applications.[18] In contrast to other photoactive materials, e.g. ZnO and TiO_2, it has a reduced band gap of 2.15 eV and is able to harvest a much larger fraction of the solar radiation on earth. Moreover, its electronic structure is suitable for photo-induced water splitting and supports the hydrogen-evolution reaction. Our group has recently developed a thin-film model system for Cu_2O(111), prepared by reactive Cu deposition on an Au(111) single crystal.[19] Its surface shows long-range hexagonal order with 6 Å periodicity and is likely Cu-deficient. STM measurements revealed the development of quasi-amorphous water ad-layers upon D_2O exposure at 90 K and subsequent annealing.[20] In this work, we complement this information with FTIR and thermal desorption (TDS) data and compare D_2O adsorption to Cu_2O with the one to bare Au(111). Although water binding is weak in both cases, the character of emerging water layers is rather different. Whereas Cu_2O features hydrophilic properties, the gold acts as a hydrophobic support.

2 Experimental Methods

The experiments have been carried out in two UHV chambers, equipped with a custom-built Beetle-type STM, TDS and low-energy electron diffraction (LEED) in one case, and with a Bruker IFS 66v/S infrared spectrometer, LEED and TDS in the other. The comparability of sample preparation in both chambers was ensured by matching LEED and TDS results, while STM and FTIR were available as complementary methods. Temperature control of the sample during TDS and FTIR measurements was realized by direct current heating in conjunction with LN_2 cooling. The TDS heating rate was set to 3 K/s. The STM images were taken in the constant current mode at 90 K.

Cu_2O films of about 3 ML thickness were prepared by Cu deposition from an e-beam evaporator in 5×10^{-6} mbar O_2, followed by 600 K annealing at UHV conditions. The crystallinity of the ad-oxide was shown by a sharp (2×2) LEED pattern with respect to Au(111).[19] The adsorption studies were performed with laboratory grade D_2O, dosed at 90 K onto the surface. In flashing experiments, the sample was heated to a preset temperature and cooled back to 90 K before data acquisition. The samples for STM have always been flashed to 155 K to remove water multilayers.

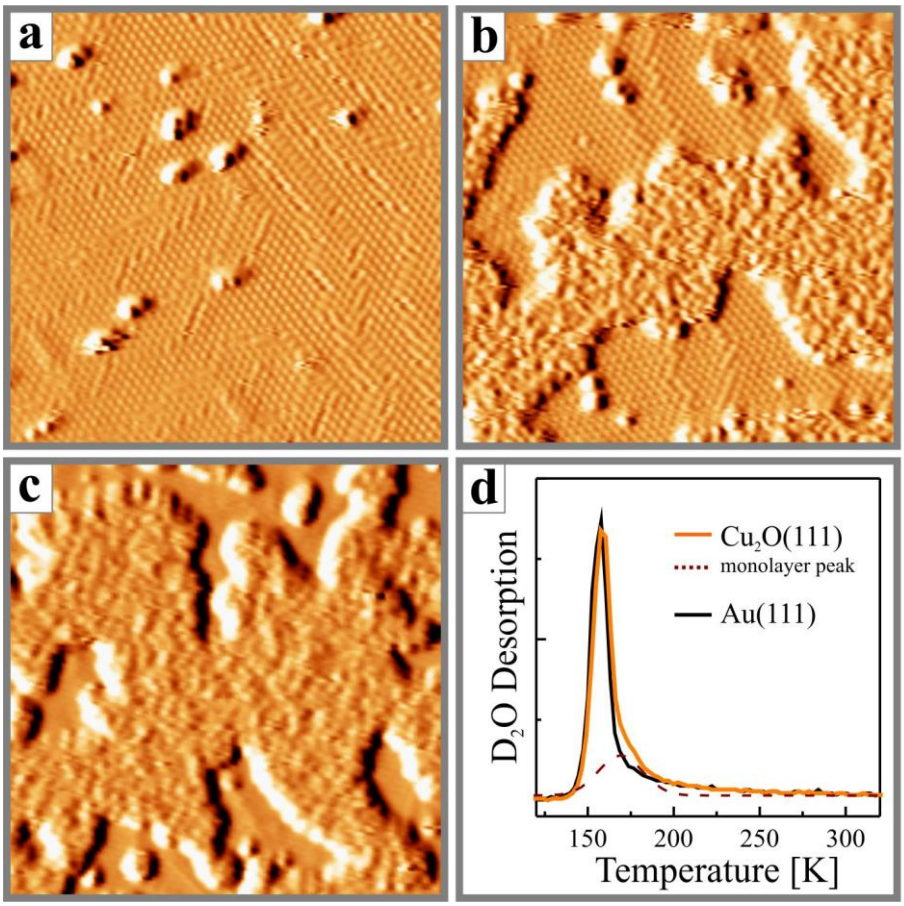

Fig. 1: (a-c) STM topographic images of Cu_2O/Au(111) thin films covered with increasing amounts of D_2O (1.0 V, 10 pA, 25 × 25 nm^2). Isolated water clusters, as detected at low coverage, evolve to amorphous islands of monolayer height at continued dosing. **(d)** Thermal desorption spectra of D_2O bound to thin Cu_2O films (orange) and Au(111) (black). The faint 170 K shoulder in the Cu_2O spectrum arises from interfacial water with slightly enhanced adhesion (broken line).

3 Results and Discussion

3.1 D_2O on Cu_2O(111)

Figure 1 displays STM topographic images of the Cu_2O/Au(111) thin film exposed to increasing amounts of water. The hexagonal structure of the oxide surface with 6 Å periodicity is clearly discernable. According to DFT calculations, the bright pattern is produced either by the *4s* dangling-bond states of unsaturated Cu_{Cus} ions in the stoichiometric surface, or by upward-buckled O_{cus} ions on Cu-deficient films.[21] Our films are likely non-stoichiometric and oxygen-terminated, as the Cu_{Cus} ions

become thermodynamically unstable in the thin-film limit. Further information on the Cu_2O/Au(111) system can be found in earlier publications.[19,20,21] At low D_2O coverage, isolated water clusters are observed that nucleate at defect lines and step edges of the Cu_2O surface (Fig. 1a). With increasing exposure, they evolve to monolayer-high islands that seem disordered at first glance (Figs. 1b and c). Closer inspection reveals however a distinct short-range order of the D_2O molecules that follows the hexagonal Cu_2O(111) lattice.[20] Evidently, the cuprous oxide exerts a weak, yet discernable template effect onto the water. TDS measurements corroborate our STM data (Fig. 1d). At low D_2O exposure, a desorption peak becomes visible at 170 K, being assigned to the water monolayer seen in STM. At higher dosing, multilayers of ASW condense on the Cu_2O surface and produce a prominent maximum at 155 K. This low-temperature desorption is of zero-order and characteristic for physisorbed water.[1,22]

Further information on the D_2O/Cu_2O adsorption system comes from FTIR. The coverage-dependent spectra in Fig. 2a display three maxima, a sharp peak at 2730 cm^{-1}, and two broad bands at about 2540 and 1210 cm^{-1}, respectively (Table 1). Whereas the former matches the frequency of the free-OD stretch mode, the latter are typical for the bound-OD stretch and the D_2O bending modes. The large width of the central peak is caused by the overlap of multiple vibrational bands and indicative for various OD-O binding lengths and angles in the amorphous water layer. It therefore corroborates the pronounced structural disorder of D_2O monolayer islands detected in the STM.[20] The emergence of the broad 2540 cm^{-1} band already at lowest exposure also points to the absence of distinct D_2O adsorption sites, in agreement with an oxygen-terminated Cu_2O(111) surface. At continued dosing, all three peaks grow in intensity without changing their energy position or width. Apparently, the disordered nature of the interfacial water is maintained in subsequent layers. However, the relative weight of the peaks undergoes certain changes. While the area ratio between free (2730 cm^{-1}) and bound-OD peaks (2540 cm^{-1}) amounts to 0.14 at sub-monolayer D_2O coverage, it decreases to 0.02 in 3 ML thick films. A more prominent free-OD peak implies a higher number of proton-bound molecules with one OD pointing towards the vacuum. Not surprisingly, this ratio is higher in the first than in subsequent D_2O layers, as the molecules get embedded into the hydrogen-bonded network. We will pick up this result again when analyzing similar data obtained on bare Au(111). In summary, the FTIR spectra strongly suggest the development of an ASW film on the cuprous oxide surface.

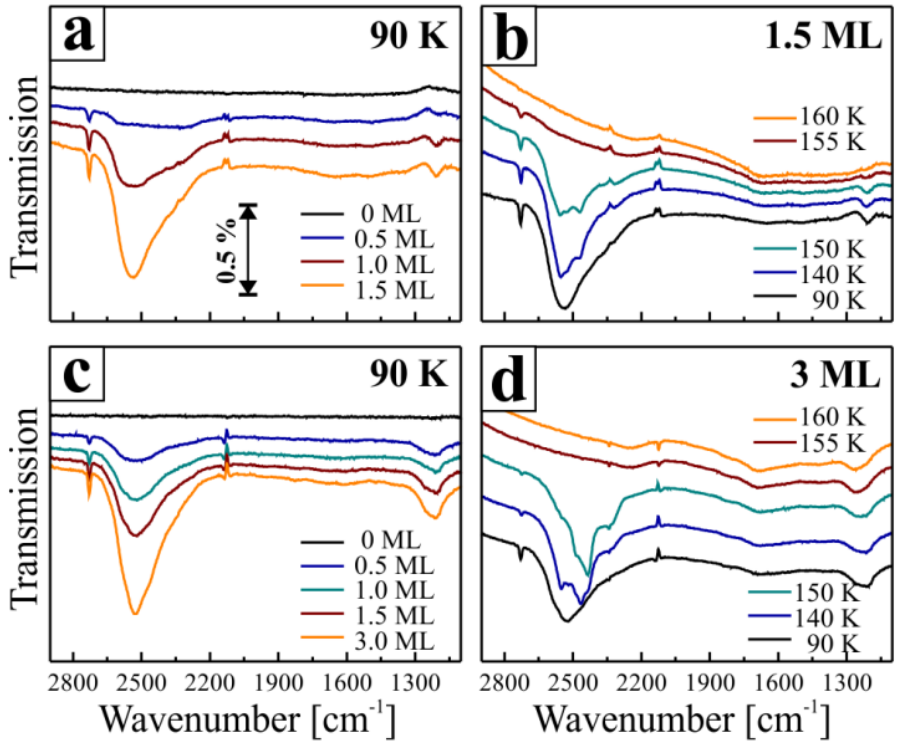

Fig. 2: FTIR spectra of D_2O on Cu_2O/Au(111) taken as a function of (a) coverage and (b) temperature. Three water related bands are discernable at 2730 cm^{-1} (free-OD stretch), 2540 cm^{-1} (bound-OD) and 1210 cm^{-1} (D_2O bending). Intensity around 2100 cm^{-1} results from residual CO bound to the surface.[23] (c,d) Identical measurements for D_2O on bare Au(111). Note the sharpening (b) and the sharpening plus redshift (d) of the broad 2540 cm^{-1} band due to structural reorganization of the water ad-layer upon annealing.

The desorption behavior of D_2O has been probed by stepwise annealing of the sample to elevated temperature and acquiring FTIR spectra after cooling back to 90 K. A spectral series taken across the D_2O desorption peak is shown in Fig. 2b. As expected, the integrated spectral intensity decreases steeply above 150 K, the onset temperature of water desorption, and has lost more than 90% of its initial magnitude at 155 K. In addition, the broad band centered at 2540 cm^{-1} sharpens across the temperature ramp and develops two distinct maxima at 2469 and 2556 cm^{-1} (Table 1). These modes can be assigned to the lower symmetric and the higher asymmetric OD frequency, as the main sub-bands of the bound-OD stretch vibrations.[9] A sharpening of the bands provides evidence for a partial ordering in the water layer, triggered by thermally stimulated reorganization of the hydrogen-bonded network.[12] However, the water layer does not crystallize upon annealing as almost no redshift of the vibrational modes is revealed. Such a redshift that might be as large as 100 cm^{-1} for bound-OD modes[4,11,12] is

however representative for a transition to crystalline ice. Crystallization of water seems thus impeded on the Cu_2O surface at temperatures below D_2O desorption. The area ratio between free and bound-OD modes finally provides insight into the fraction of low-coordinated, probably upright standing D_2O molecules during annealing. Opposite to the adsorption series, this number increases from 0.02 to 0.09 and especially the final traces just before D_2O removal are characterized by an intense free-OD peak (Table 1). Apparently, the remaining molecules adopt an upright, proton-bound configuration on the Cu_2O surface again.

3.2 D_2O on Au(111)

To identify peculiarities in the water adsorption behavior on cuprous oxide, similar data has been acquired on bare Au(111) that serves as substrate for oxide growth. The comparison with Cu_2O spectra is meaningful at this point, as gold exhibits similar coupling strength to water according to TDS (Fig. 1d). Also on Au(111), the most prominent TDS peak lies at 155 K and is assigned to ASW desorbing from the surface. However, the faint 170 K shoulder observed for Cu_2O is missing in the gold spectra. Apparently, interfacial water does not experience enhanced adhesion to the metal surface.

Despite difference in the TDS data, the FTIR signatures of water bound to $Cu_2O(111)$ and Au(111) surfaces are surprisingly similar (Fig. 2). In fact, spectra taken at increasing exposure are nearly indistinguishable. The spectra on gold are governed by a sharp free-OD line at 2730 cm^{-1}, and broad absorption maxima at 2530 cm^{-1} and 1210 cm^{-1}, assigned to the bound-OD stretch and the D_2O bending modes, respectively (Table 1). The large width of the central band indicates again low structural order in the water layer and proves the development of ASW also on Au(111). A main difference is however the area ratio between free and bound-OD stretch vibrations that amounts to ~0.025 independent of water coverage. Note that similar values have been obtained for thick ASW layers on Cu_2O, while the ratio dropped by a factor of five for D_2O monolayers on the oxide surface. Apparently, the number of low-coordinated, upright standing D_2O molecules with unperturbed OD vibrations is much higher on Cu_2O, suggesting pronounced differences in the water-surface interaction with respect to gold.

Additional deviations are observed in temperature-controlled FTIR spectra, as shown in Fig. 2d. As on Cu_2O, the overall spectral intensity diminishes drastically across the water desorption peak. The process is accompanied by a sharpening of the broad central band that splits into 2436 and 2486 cm^{-1} modes for the symmetric and asymmetric OD stretch vibration, respectively. In contrast to the Cu_2O case, the bands undergo a pronounced redshift upon annealing, suggesting that the ad-water not only improves structural order but transforms largely to crystalline ice. The observed redshift of the bound-OD frequencies results from enhanced inter- with respect to intramolecular coupling in the D_2O network. Further support for a D_2O crystallization on Au(111) above 150 K comes from the nearly complete suppression of the free-OD peak, despite large residual intensity in the bound-OD region (area ratio below 0.01). Evidently, almost all low-coordinated water molecules have disappeared from the surface, as water condenses into large 3D ice clusters with low surface to volume ratio. The different trends in the annealing behavior of ASW on $Cu_2O(111)$ and Au(111) are rationalized in the final paragraph of our paper.

3.3 Discussion

As presented above, ASW layers develop on both, thin-film $Cu_2O(111)$ and metallic Au(111) surfaces upon water dosing at low temperature. In the case of $Cu_2O(111)$, we have recently assigned this behavior to a nonstoichiometric and oxygen-rich surface termination that lacks low-coordinated Cu_{Cus} ions.[20] The latter would enable strong covalent bonding of D_2O, whereas only weak hydrogen interactions are present in the absence of Cu_{cus}. In fact, the oxygen-terminated Cu_2O surface is neither able to dissociate incoming water molecules nor to trigger their long-range ordering, in agreement with our data and theoretical results.[24] Also, the 3Å periodicity of the oxygen sub-lattice in $Cu_2O(111)$ impedes the development of a regular hydrogen-bonded network. Molecular interaction lengths in fully relaxed water layers amount to 2.4-2.8 Å; 0.8 Å for the O-D bond inside the molecule and 1.6-2.0 Å for the hydrogen bond to its neighbor.[2,4] On $Cu_2O(111)$, this spacing needs to be increased by about 20% in order to reach registry at the water-oxide interface. Both factors, the weak adhesion and the unfavorable lattice match are responsible for ASW formation on Cu-deficient $Cu_2O(111)$ even at low coverage.

Note that water binding to O-terminated cuprous oxide also explains the high density of proton-bound D_2O molecules, as concluded from the large area ratio between free and bound-OD vibrational bands. The associated molecules likely bind in a D-down configuration to the O_{cus} ions and to a smaller extent to defects and step edges in the oxide surface.

Water adsorption to closed-packed Au(111), on the other hand, is entirely governed by physisorptive interaction schemes, mostly van-der-Waals coupling. Main reasons are the high electronegativity and the delocalized electronic structure of gold that repels the water-oxygen and inhibits formation of localized bonds to the D_2O molecules, respectively. As a consequence, Au(111) supports formation of ASW, although crystalline water structures have been found on more electropositive *d*-metals, e.g. Ru(0001) and Cu(111).[2] Also, the low area ratio between free and bound-OD stretch vibrations is compatible with a mainly physisorptive interaction scheme, in which the molecules lie flat on the Au(111) surface in order to maximize van-der-Waals bonding.

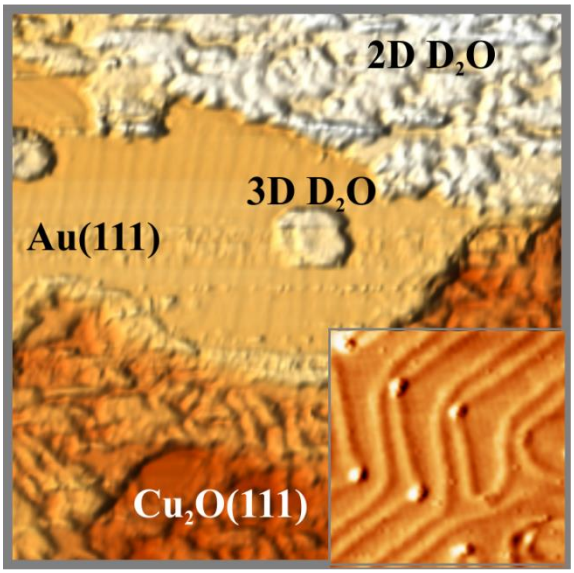

Fig. 3: STM image of D_2O bound to Cu_2O/Au(111) after flashing to 155 K (1 V, 10 pA, 150 × 150 nm^2). While the ASW layer remains intact on the oxide surface, dewetting and formation of 3D ice clusters occurs on the metal. The inset shows preferential D_2O nucleation at elbows of the Au herringbone reconstruction (35 × 35 nm^2)

Although formation of ASW has been found on both, Cu_2O(111) and Au(111), the water desorption behavior is distinctively different on the two supports. While on the oxide film, the water ad-layer only partially reorganizes upon annealing, dewetting and crystallization is observed on gold. The latter conclusion is drawn from the sharpening and redshift of vibrational bands in the bound-OD region (2530 cm^{-1}), but can be seen also in real-space STM data. A respective image is depicted in Fig. 3 and shows a mixed Cu_2O-Au(111) surface after water adsorption and annealing close to the desorption tempera-

ture. The bare Au(111), clearly discernable by its herringbone reconstruction, holds only few 3D ice clusters that typically attach to the elbows of the reconstruction (Fig. 3, inset).[25] Conversely, the adjacent Cu_2O regions are entirely covered by ASW and no signs for dewetting and crystallization are found. Note that STM is unable to resolve small structural changes in ASW films, although these are obvious in the FTIR data.

The pronounced differences in water desorption can be boiled down to the hydrophilic versus hydrophobic nature of the two model systems, being probed at the molecular scale here. Despite a weak overall adhesion, $Cu_2O(111)$ shows clear signs of hydrophilicity as the water remains bound to the surface up to the desorption temperature. Au(111), on the other hand, is hydrophobic as actual water desorption is preceded by a dewetting step. While the hydrophilicity of $Cu_2O(111)$ is assigned to hydrogen bonding between the surface-oxygen and the water-hydrogen, the hydrophobicity of Au(111) mainly relates to repulsive forces between water-oxygen and the electronegative gold. Similar differences have been observed for other systems,[26] e.g. bare versus mica-covered Pt(111),[4] and stoichiometric versus hydroxylated MgO.[27] Whereas oxygen-terminated surfaces often feature hydrophilic properties,[28] many metals are hydrophobic and promote the formation of 3D ice clusters.[3,17]

4 Conclusion

The adsorption behavior of D_2O to $Cu_2O(111)$ and metallic Au(111) has been compared. Layers of ASW develop on both surfaces at 90 K, as demonstrated by characteristic FTIR spectra and STM data. For the D_2O/Cu_2O system, a high-temperature shoulder in TDS reflects the formation of interfacial water with enhanced adhesion. This layer is unable to undergo structural ordering upon annealing even close to the desorption temperature of 170 K. In contrast, the ASW on Au(111) dewets and aggregates to larger ice clusters from which desorption takes place. The deviating desorption schemes reflect the hydrophilic versus hydrophobic nature of oxide and metal surfaces, respectively, whereby the hydrophilicity of $Cu_2O(111)$ arises from an efficient hydrogen bonding of water to the surface O ions. Further experiments will explore whether water binding to cuprous oxide can be tailored by preparing Cu-

rich instead of O-rich surface terminations. In this case, much higher desorption temperatures and the development of crystalline water layers would be expected.

Tab.1: *Compilation of frequencies and intensities of prominent D_2O vibrational bands detected in FTIR. The area ratio of free and bound-OD peaks was determined by integrating the intensity course between 2710-2740 and 2400-2700 cm^{-1}, respectively.*

Dosage/ Temperature	**Free-OD [cm^{-1}]**	**Bound-OD [cm^{-1}]**		**D_2O Bending [cm^{-1}]**	**Area ratio free/bound OD**
		symmetric	asymmetric		
$Cu_2O(111)$					
0.5 ML, 90 K	2730	2350-2550		--	0.14
1.5 ML, 90 K	2730	2540		1210	0.02
1.5 ML, 140 K	2730	2476	2554	1210	0.015
1.5 ML, 150 K	2730	2469	2556	1210	0.02
1.5 ML, 155 K	2730	--		1210	0.09
Au(111)					
0.5 ML, 90 K	2730	2530		1220	0.03
3 ML, 90 K	2730	2530		1210	0.02
3 ML, 140 K	2730	2465	2551	1230	0.007
3 ML, 150 K	2730	2436	2486	1240	0.009
Reference [29]					
D_2O, gas		2672	2788	1178	
D_2O, liquid		2407	2476	1206	

5 Acknowledgements

The authors are grateful for financial support via the DFG grant 'Photocatalytic processes probed at the atomic scale'. F. Stavale thanks the FAPERJ and the CNPq for financial support.

6 References

[1] Henderson, M. A.; Interaction of Water with Solid Surfaces: Fundamental Aspects, Surf. Sci. Rep. **2002**, *46*, 1-308.

[2] Hodgson, A.; Haq, S. Water Adsorption and the Wetting of Metal Surfaces. *Surf. Sci. Rep.* **2009**, *64*, 381–451.

[3] Carrasco, J.; Santra, B.; Klimes, J.; Michaelides, A. To Wet or Not to Wet? Dispersion Forces Tip the Balance for Water Ice on Metals, *Phys. Rev. Lett.***2011,** *106*, 026101.

[4] Verdaguer, A.; Sacha, G. M.; Bluhm, H.; Salmeron, M. Molecular Structure of Water at Interfaces: Wetting at the Nanometer Scale. *Chem. Rev.* **2006**, *106*, 1478–1510.

[5] Cappus, D.; Xu, C.; Dillmann, E. B.; Ventrice, J. C. a.; Shamery, K. Al; Kuhlenbeck, H.; Freund, H.-J. Hydroxyl Groups on Oxide Surfaces : NiO (100), NiO (111) and Cr_2O_3(111). *Chem. Phys.* **1993**, *177*, 533–546.

[6] Hagen, W.; Tielens, A. G.; Greenberg, J. M. The Infrared Spectra of Amorphous Solid Water and Ice Ic between 10 and 140 K. *Chem. Phys.* **1981**, *56*, 367–379.

[7] Sivakumar, T. C.; Schuh, D.; Scegats, M. G.; Rice, S. A. The 2500-4000 cm^{-1} Raman and Infrared Spectra of Low Density Amorphous Solid Water and Polycrystalline Ice I. *Chem. Phys. Lett.* **1977**, *48*, 212–218.

[8] Buch, V.; Devlin, J. P. A New Interpretation of the OH-Stretch Spectrum of Ice. *J. Chem. Phys.* **1999**, *110*, 3437.

[9] Li, F.; Skinner, J. L. Infrared and Raman Line Shapes for Ice Ih. II. H2O and D 2O. *J. Chem. Phys.* **2010**, *133*.

[10] Bakker, H. J.; Skinner, J. L. Vibrational Spectroscopy as a Probe of Structure and Dynamics in Liquid Water, Chem. Rev. **2010,** *110*, 1498-1517.

[11] Backus, E. H. G.; Grecea, M. L.; Kleyn, A. W.; Bonn, M. Surface Crystallization of Amorphous Solid Water. *Phys. Rev. Lett.* **2004**, *92*, 236101.

[12] Shephard, J. J.; Evans, J. S. O.; Salzmann, C. G. Structural Relaxation of Low-Density Amorphous Ice upon Thermal Annealing. *J. Phys. Chem. Lett.* **2013**, *4*, 3672–3676.

[13] Maier, S.; Lechner, B. a. J.; Salmeron, M. Growth and Structure of the First Layers of Ice on Ru(0001) and Pt(111). *J. Am. Chem. Soc.* **2016**, jacs.5b13133.

[14] Parkinson, G. S. Iron Oxide Surfaces. *Surf. Sci. Rep.* **2016**, *71*, 272–365.

[15] Zhao, X.; Shao, X.; Fujimori, Y.; Bhattacharya, S.; Ghiringhelli, L. M.; Freund, H. J.; Sterrer, M.; Nilius, N.; Levchenko, S. V. Formation of Water Chains on CaO(001): What Drives the 1D Growth? *J. Phys. Chem. Lett.* **2015**, *6*, 1204–1208.

[16] Morgenstern, M.; Müller, J.; Michely, T.; Comsa, G.; The Ice Bilayer on Pt(111): Nucleation, Structure and Melting, Z. Phys.Chem,. **1997**, *198*, 43-72.

[17] Michaelides, A.; Morgenstern, K. Ice Nanoclusters at Hydrophobic Metal Surfaces. *Nat. Mater.* **2007**, *6*, 597–601.

[18] Meyer, B. K.; Polity, a.; Reppin, D.; Becker, M.; Hering, P.; Klar, P. J.; Sander, T.; Reindl, C.; Benz, J.; Eickhoff, M.; et al. Binary Copper Oxide Semiconductors: From Materials towards Devices. *Phys. Status Solidi* **2012**, *249*, 1487–1509.

[19] Sträter, H.; Fedderwitz, H.; Groß, B.; Nilius, N. Growth and Surface Properties of Cuprous Oxide Films on Au(111). J. Phys. Chem. C **2015**, 119, 5975−5981.

[20] Möller, C. ; Nilius, N. Water Adsorption on Cu_2O(111) Surfaces: A STM Study, J. Phys. Chem. C **2017**, *121*, 20877-20881.

[21] Nilius, N.; Fedderwitz, H.; Groß, B.; Goniakowski, J.; Noguera, C. Incorrect DFT- GGA Predictions of the Stability of Non-Stoichiometric/Polar Dielectric Surfaces, Phys. Chem. Chem. Phys. **2016,** 18, 6729−6733.

[22] Henderson, M. An HREELS and TPD Study of Water on TiO_2(110): The Extent of Molecular versus Dissociative Adsorption, Surf. Sci. **1996**, 355, 151−166.

[23] The FTIR feature at ~2120 cm^{-1} is assigned to CO adsorption from the residual gas. CO quickly populates suitable binding sites on Cu_2O and therefore contributes already to reference spectra of the bare sample. Upon water exposure, D_2O replaces the weakly bound CO and respective bands show up as negative absorption.

[24] Riplinger, C.; Carter, E. A. Cooperative Effects in Water Binding to Cuprous Oxide Surfaces. *J. Phys. Chem. C* **2015**, *119*, 9311–9323.

[25] Gawronski, H.; Morgenstern, K.; Rieder, K. H. Electronic Excitation of Ice Monomers on Au(111) by Scanning Tunneling Microscopy: Vibrational Spectra and Induced Processes. *Eur. Phys. J. D* **2005**, *35*, 349–353.

[26] Dohnálek, Z.; Ciolli, R. L.; Kimmel, G. a.; Stevenson, K. P.; Smith, R. S.; Kay, B. D. Substrate Induced Crystallization of Amorphous Solid Water at Low Temperatures. *J. Chem. Phys.* **1999**, *110*, 5489.

[27] Fujimori, Y.; Zhao, X.; Shao, X.; Levchenko, S. V.; Nilius, N.; Sterrer, M.; Freund, H. J. Interaction of Water with the CaO(001) Surface. *J. Phys. Chem. C* **2016**, *120*, 5565–5576.

[28] Henderson, M.; Chambers, S. HREELS, TPD and XPS Study of the Interaction of Water with the Cr_2O_3(001) Surface. *Surf. Sci.* **2000**, *449*, 135.

[29] Pang, X. F., Water: Molecular Structure and Properties, (New Jersey, 2014, World Scientific).

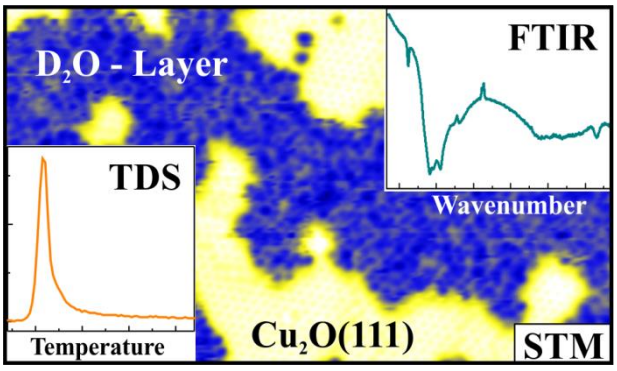
D2O - Layer
FTIR
Wavenumber
TDS
Temperature
Cu2O(111)
STM